



Abrupt warming and alpine glacial retreat through the last deglaciation in Alaska interrupted by modest Northern Hemisphere cooling

Joseph P. Tulenko^{1,2}, Jason P. Briner², Nicolas E. Young³, and Joerg M. Schaefer³

5 ¹Berkeley Geochronology Center, 2455 Ridge Road, Berkeley, CA 94709

²Department of Geology, University at Buffalo, 126 Cooke Hall, Buffalo, NY 14260

³Lamont-Doherty Earth Observatory, Columbia University, 61 Route 9W, Palisades, NY 10964

Correspondence to: Joseph P. Tulenko (jtulenko@bgc.org)

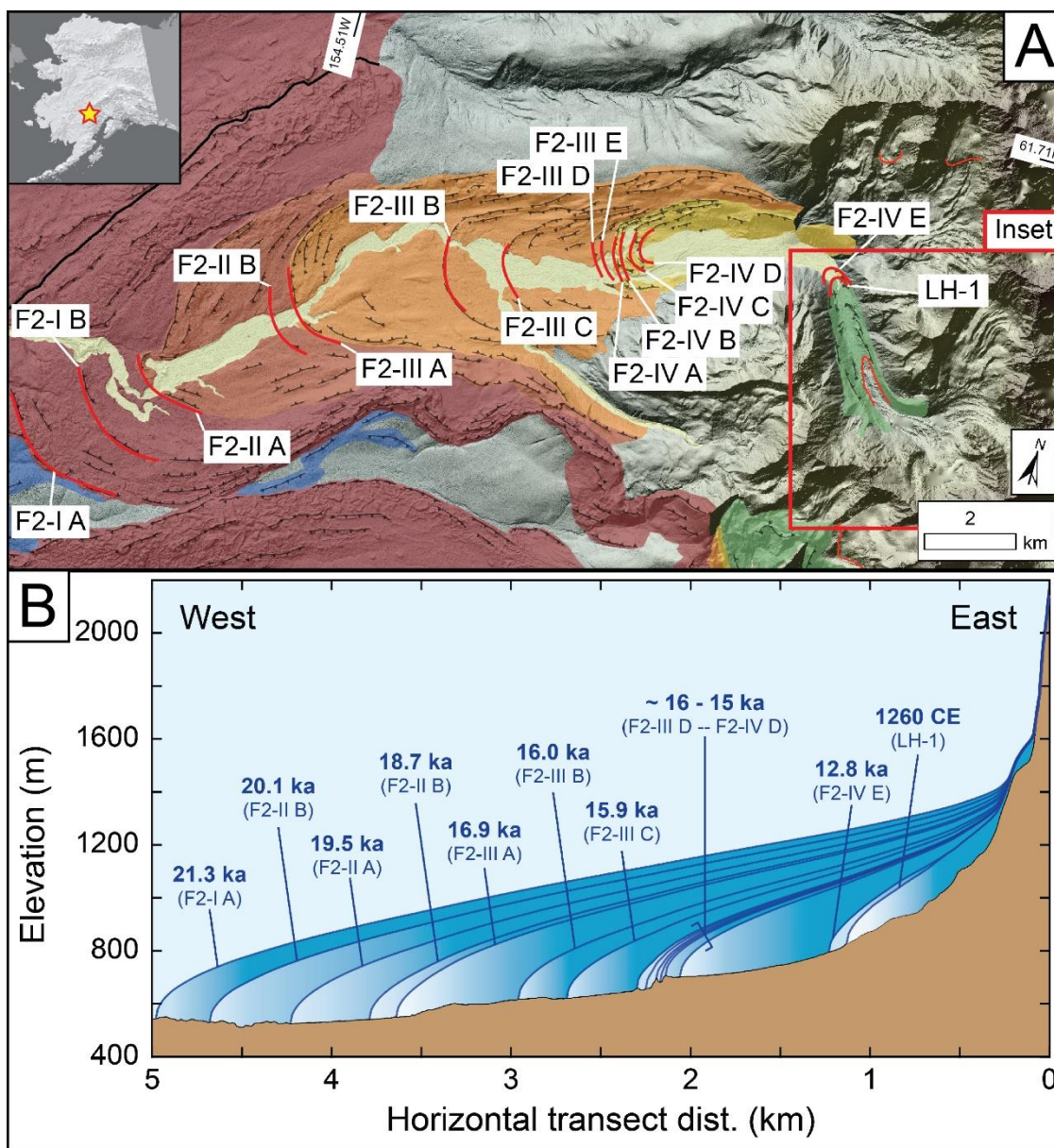
Abstract. Alpine glacier-based temperature reconstructions spanning the last deglaciation provide critical constraints on local-to-regional climate change and have been reported from several formerly glaciated regions around the world yet remain sparse from high northern latitude regions. Using newly and previously ¹⁰Be-dated moraines, we report paleo-glacier equilibrium line altitudes (ELA) for 15 time slices spanning the Last Glacial Maximum (LGM) to the Little Ice Age (LIA) for a valley in the western Alaska Range. We translate our ELA reconstructions into a proxy for summer temperature by applying a dry adiabatic lapse rate at each reconstructed ELA relative to the outermost LIA moraine. We observe ~4°C warming through the last deglaciation at our site that took place in two steps following initial gradual warming: ~1.5°C abrupt warming at 16 ka, ~2 kyr after global CO₂ rise, and ~2° C warming at ~15 ka, near the start of the Bølling. Moraine deposition and modest summer cooling during Heinrich Stadial 1 and the early Younger Dryas (YD) suggest that despite these events expressing more strongly in wintertime, the classic blueprint of North Atlantic climate variability extends to the western Arctic region.

20 **1 Introduction**

Global mountain glacier recession is one of the clearest indicators of modern planetary warming (Hugonnet et al., 2021). Paleo-data suggest that alpine glaciers are highly sensitive to temperature changes on both centennial (Roe et al., 2017) and millennial time scales (Schaefer et al., 2006). The last deglaciation (~19 – 11 ka) contains periods of abrupt warming akin to contemporary climate change – particularly later in the interval during the ‘late glacial’ ~15-11 ka – and considerable effort has been spent to constrain the timing and pace of mountain glacier fluctuations world-wide through this interval (e.g., Putnam et al., 2013; Ivy-Ochs, 2015; Palascios et al., 2020). However, mountain glacier fluctuations in the high northern latitudes – in locations where ice sheets were largely absent or restricted– are less well characterized due in part to the limited availability of suitable sites for organic radiocarbon dating, which presents a significant challenge compared to more temperate regions (Wittmeier et al. 2020).



30



35

Figure 1. A: Geomorphic map of the North Swift River valley with reconstructed moraine positions denoted (n = 15). Inset: starred location of the Revelation Mountains in Alaska. B: Schematic of alpine glacier retreat in the North Swift River valley that includes moraine ages reported here and in Tulenko et al. (2022). Panel A source: ArcticDEM product available from the University of Minnesota Polar Geospatial Center. Inset map source: IBCAO product available from GEBCO.

Glacier equilibrium line altitudes (ELAs) are a representative measure of the climatic conditions supporting a glacier. Climate-driven positive and negative mass balance changes force the ELA to lower or rise, respectively (Ohmura et al.,



1992; Oerlemans et al., 2005, Braithewaite, 2008). Reconstructing paleo glaciers through detailed mapping and dating
40 techniques provides valuable data for estimating paleo-ELAs, which serve as a powerful paleoclimate proxy for glaciated
regions. Improved access to accurate digital elevation models (DEMs) and the development of semi-automated paleo-glacier
surface and ELA reconstruction tools (Pellitero et al., 2015, 2016) paves a path for more objective measures of paleo-ELA
calculation. Changes in ELA are dependent primarily on summer (JJA) temperatures and annual snowfall (Oerlemans et al.,
2005). Some studies suggest, however, that in most environments other than the most extremely arid environments such as
45 modern-day inner Mongolia, alpine glacier ELAs are dominated by summer temperatures (e.g., Rupper and Roe, 2008).

Building on a recently published ^{10}Be chronology of 14 moraines in the North Swift River valley, Revelation Mountains,
western Alaska Range (Tulenko et al., 2018, 2022), we constrain additional ^{10}Be ages for three late Holocene moraines in the
valley and generate a paleo-ELA based proxy summer temperature record from our site. We estimate the timing and pace of
50 warming through the last deglaciation by transforming ΔELAs into summer temperature assuming a dry adiabatic lapse rate
of $10^\circ\text{C}/\text{km}$. The magnitude of temperature change we obtain is supported by independent climate proxy records in Alaska,
and we compare our record with other glacier-based temperature reconstructions to speculate about the controls on climate in
Alaska through deglaciation.

2. The Revelation Mountains field site

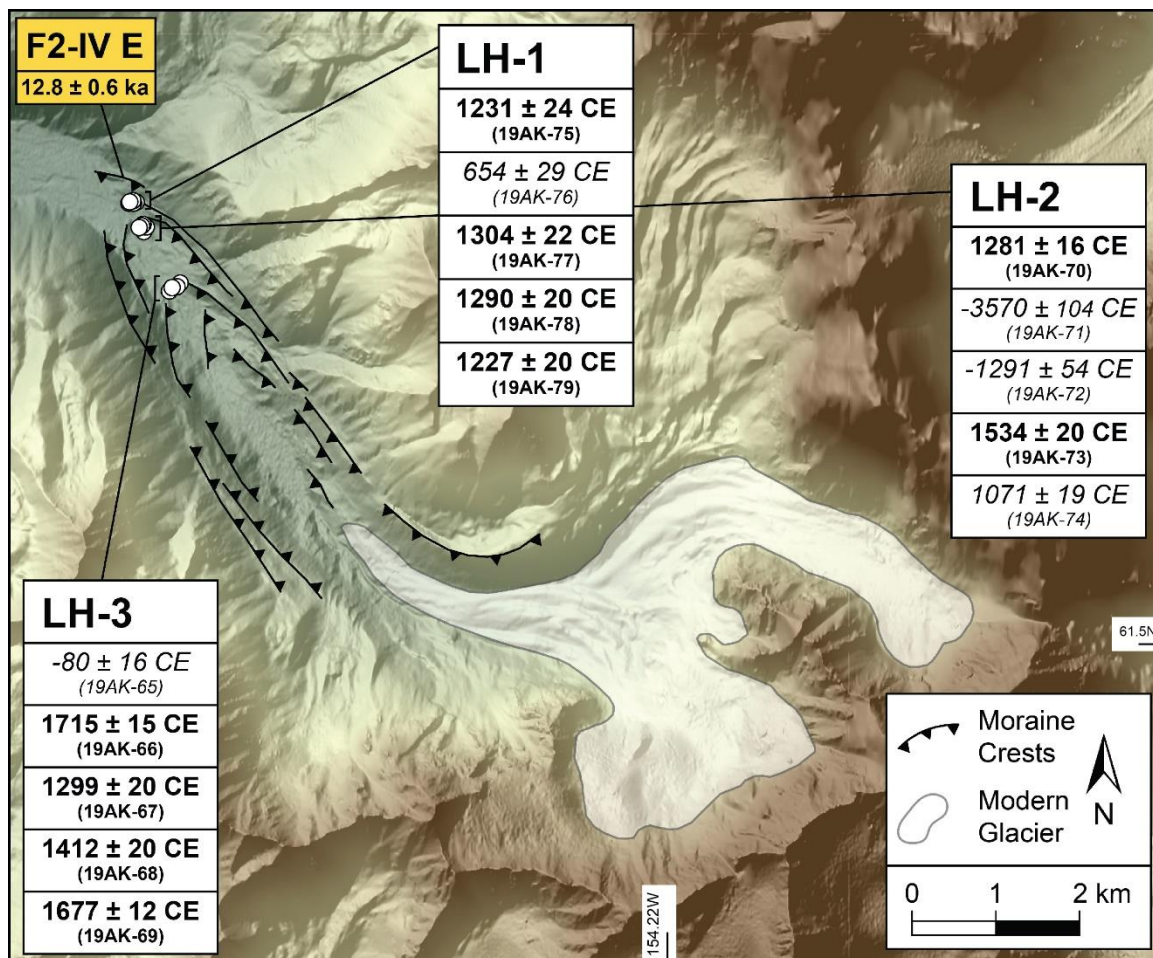
55 The Revelation Mountains field site is located on the western limb of the Alaska Range (Fig. 1 inset) where dense sequences
of moraines deposited by alpine glaciers fluctuating through the last deglaciation are well-preserved. The Revelation
Mountains are cored by a granitic pluton, and large tabular boulders deposited on moraines are suitable targets for
cosmogenic ^{10}Be exposure dating. The site is located far South from seismic activity along the Denali Fault, and thus
moraines deposited in these valleys have likely remained more stable after deposition compared to moraines in locations
60 more proximal to the Denali Fault system (e.g., Briner et al., 2005; Matmon et al., 2006; Dortch et al., 2010). All these
factors have led to productive chronologic constraints on deglaciation in Alaska (Tulenko et al., 2022).

Within the Revelation Mountains, the North Swift River valley hosts the densest and most comprehensive sequence of
moraines of any valley surveyed at our site (Fig. 1). For more details on the mapping and dating approaches used to generate
65 the deglacial chronology in the North Swift River valley site, readers are referred to Tulenko et al. (2022). After a thorough
moraine dating campaign of deglacial moraines in the valley, we further surveyed moraines in the valley deposited near the
terminus of the extant glacier in the valley that were likely late Holocene in age (Fig. 2). For this study, the purpose was to
target late Holocene moraines to contextualize the magnitude of deglacial retreat in the North Swift River valley. Thus, all
inferred climate fluctuations reported here are relative to the late Holocene advances observed at our site.



70 3 Chronology of late Holocene glacier fluctuations in Alaska

To complete the time series of glacier retreat in the North Swift River valley, we collected surface samples for ^{10}Be dating from 15 granitic boulders on three distinct moraine crests between the innermost late glacial moraine (F2-IV E) and an unnamed extant glacier (Figs. 1 and 2). The moraines are sharp-crested, and clast supported with minimal vegetation cover (Fig. 3). We selected the largest, tabular boulders (>1-2 m tall) with horizontal-to-sub-horizontal top surfaces. Surface samples approximately 2 cm thick (see Table 1 for exact thickness measurements) and ~1 kg in mass were extracted using a Hilti brand angle grinder with diamond-tipped cutting discs and a hammer and chisel. GPS coordinates were taken with a handheld GPS, and shielding corrections were calculated using in-field measurements with a handheld clinometer and the shielding correction calculator from the online exposure age calculator website (<https://hess.ess.washington.edu/>). We targeted large, tabular boulders on clast supported moraines to minimize the likelihood that post-depositional processes – e.g., snow cover and moraine degradation – inhibited production of cosmogenic ^{10}Be in sampled surfaces, which would produce ages younger than the true timing of moraine deposition.





85 **Figure 2. Shaded relief map of the modern North Swift River valley glacier and late Holocene moraines with ^{10}Be ages displayed. Samples listed in italics are suspected outliers. Age for the F2-IV E moraine segment from Tulenko et al., 2022. Map source: 5m resolution IFSAR Alaska DEM product available from the USGS.**

90 All samples were processed from full surface sample to prepared ^{10}Be targets at the Lamont-Doherty Earth Observatory (LDEO) cosmogenic dating laboratory following procedures outlined in Schaefer et al. (2009). Beryllium measurements for samples and batch blanks were made at the Lawrence Livermore National Lab Center for Accelerator Mass Spectrometry (LLNL-CAMS). All $^{10}\text{Be}/^9\text{Be}$ ratios were standardized to the 07KNSTD standard of 2.85×10^{-12} (Nishiizumi et al., 2007), and blank-corrected final ^{10}Be concentrations are reported in Table 1 and in the ICE-D database (www.ice-d.org) along with all other relevant sample observations and measurements.

95 ^{10}Be surface exposure ages reported here were calculated on the online exposure age calculator (Balco et al., 2008) using the Baffin Bay Arctic Production rate (Young et al., 2013), and the time-dependent scaling scheme from Lal (1991) and Stone (2000). Several previous studies in Alaska have utilized this production rate calibration/scaling scheme combination (Valentino et al., 2021; Tulenko et al., 2022 and references cited therein), and the production rate measured in Baffin Bay is statistically identical to other high-latitude Northern Hemisphere calibration sites such as the Scottish Highlands Rannoch Moor site (Putnam et al., 2019), The Swiss Alps Chironico Landslide site (Claude et al., 2014), and Northeastern North America (Balco et al., 2009). Use of other commonly applied production rate calibrations would result in ages offset by ~3%. Because we sampled large tabular boulders on clast-supported moraines, we assume the tops of the boulders were wind-swept; we do not correct for snow-cover. We also do not correct for boulder surface erosion since the boulders are crystalline granitic lithology and thus resistant to weathering, particularly on the brief (hundreds of years) period between
100 deposition and sample measurement.
105

Ages from the three dated moraines situated 200-1000 m inboard of the innermost late Pleistocene (F2-IV E) moraine range from 1227 – 1715 CE ($n = 10$; not including 5 potential outliers; Fig. 1, Fig. 2, Table 1). Ages that are suspected outliers do not overlap with any other ages within two standard deviations and are older than the remaining ages, which indicates they
110 may have been influenced by nuclide inheritance. The outermost moraine (LH-1) has four ages that overlap within 2 standard deviations and average 1263 ± 60 CE. The next moraine (LH-2) does not have any ages that overlap, but one boulder age at 1281 ± 16 CE coincides with the ages from LH-1 so it is possible it was deposited inboard of the LH-1 position at the same time the LH-1 moraine formed and then was recycled during the advance that formed LH-2. For the innermost moraine dated, two of the five boulder ages overlap within 2 standard deviations and average 1696 ± 27 CE.
115 Additionally, LH-3 contains one boulder age that also conforms well with the ages from LH-1 at 1299 ± 20 CE and could have a similar history to the age from the LH-2 moraine at 1281 ± 16 CE.



120 **Figure 3. Example photos of sampled boulders on the three late Holocene moraines (top and bottom left panels). Bottom right panel is an image of the left-lateral segment of LH-3 where sampled boulders are situated. Note person on moraine crest for scale. Images of all sampled boulders can be found in the ICE-D database (www.ice-d.org).**

Many of the well-constrained observations of Little Ice Age (LIA) glacier fluctuations in Alaska come from southern Alaska, where tree-ring chronologies from trees sheared at their bases by glacial overriding tightly constrain episodes of glacier
125 advance (Figs. 4 and 5; Wiles et al., 2002, 2004; Barclay et al., 2009). These precise chronologies reveal two major glacier advances at ~1200-1300 CE and ~1600-1800 CE (Fig. 5). In comparison, we observe moraines deposited in the North Swift River valley at 1263 ± 60 CE and 1696 ± 27 CE. The coherence of ^{10}Be ages in the North Swift River valley with tree-kill dates in southern Alaska and suggests similar climate controls for glaciers in the western Alaska Range and in southern Alaska during the LIA.



130

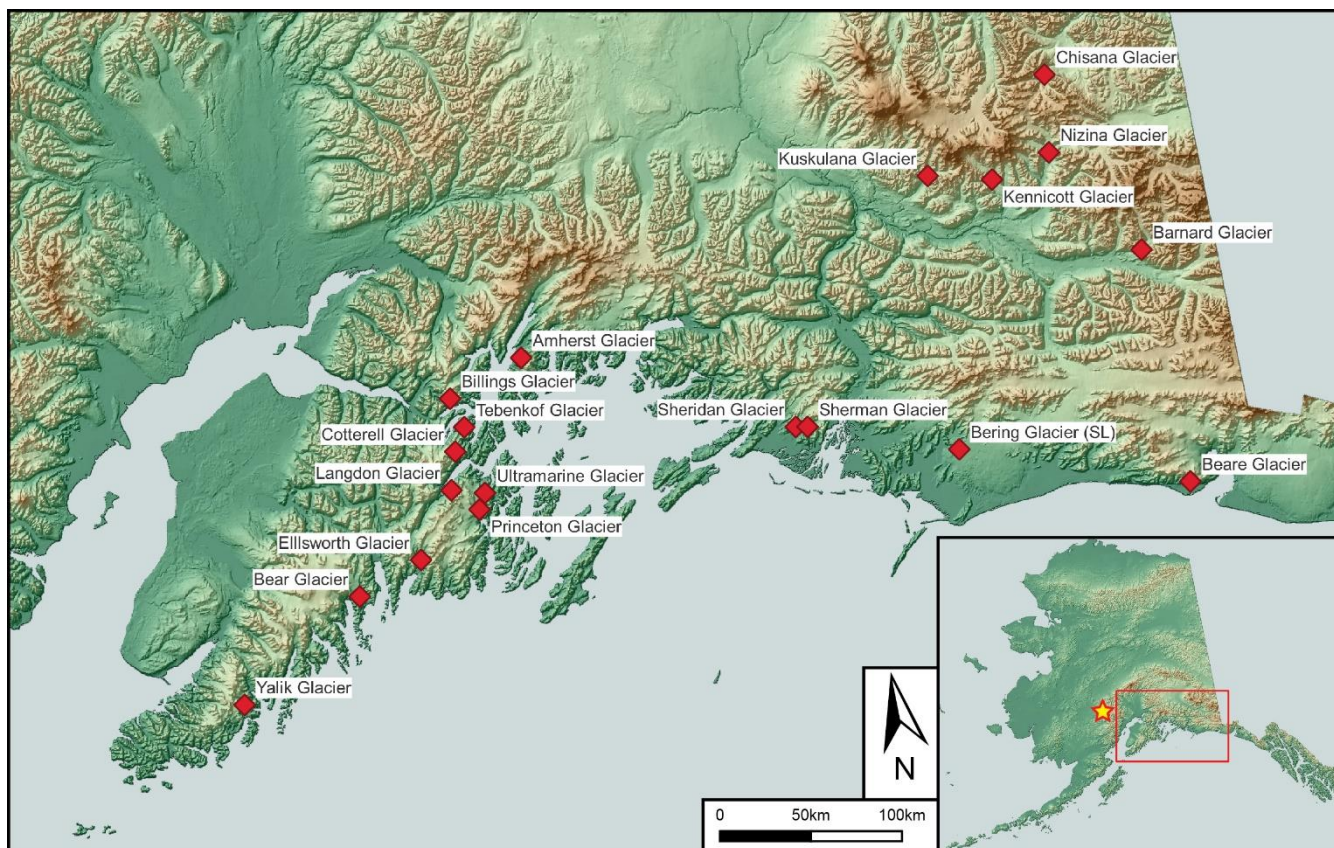
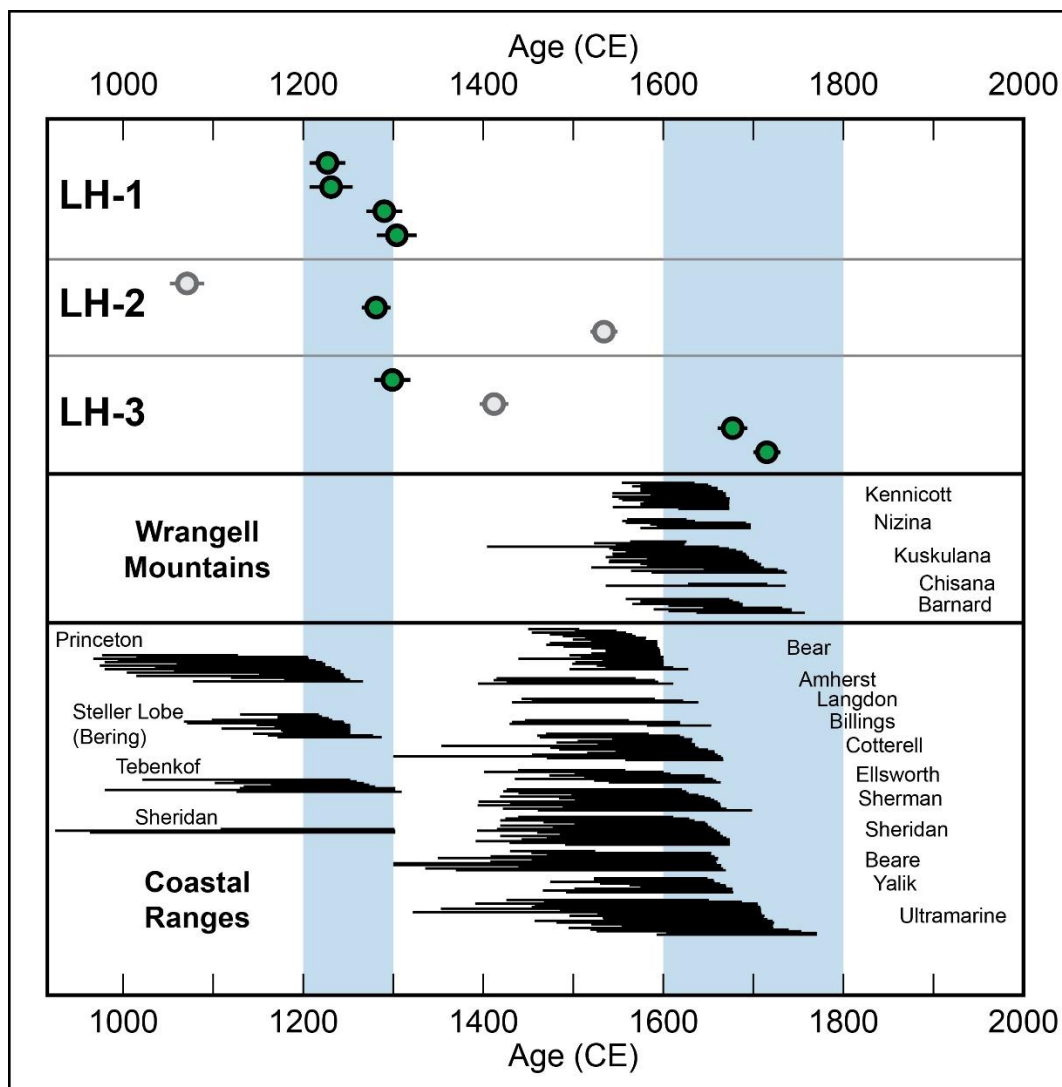


Figure 4. Locations of glaciers in Southern Alaska with well-constrained late Holocene advances from tree-kill dates. Location of the Revelation Mountains denoted by a star in the inset. Basemap available from ASTER.



135

Figure 5. Comparison of late Holocene moraine ages (green dots; grey dots are outliers) with tree-ring-based southern Alaska glacial fluctuations (black bars; Barclay et al., 2009). Light blue vertical bars indicate periods of moraine deposition in the Revelation Mountains (upper panel) and tree-kill dates signifying glacier culminations in Southern Alaska (lower panels) at ~1200-1300 CE and ~1600-1800 CE. See Fig. 4 for geographic locations of tree-kill dates.

140

Table 1. ^{10}Be age information

Sample name	Latitude (DD)	Longitude (DD)	Elevation (masl)	Thickness (cm)	Shielding Correction	Blank Ratio	[Be-10] atoms g ⁻¹	+/- atoms g ⁻¹	Age (a)	Age (CE)
LH-1										
19AK-75	61.67542	-154.28345	822	1.85	0.964221	7.685E-16	7122.050705	217.5700355	788 ± 24	1231 ± 24
19AK-76	61.67548	-154.28334	822	2.41	0.964221	7.685E-16	12222.69362	259.7289228	1365 ± 29	654 ± 29



19AK-77	61.67552	-154.28322	818	4.92	0.964221	7.685E-16	6273.866833	189.2872742	715 ± 22	1304 ± 22
19AK-78	61.67542	-154.28313	820	2.52	0.964221	7.685E-16	6535.901693	182.0415642	729 ± 20	1290 ± 20
19AK-79	61.67546	-154.28278	820	2.87	0.964221	7.685E-16	7087.088473	175.6326924	792 ± 20	1227 ± 20
LH-2										
19AK-70	61.6741	-154.28181	829	2.5	0.964221	7.685E-16	6673.440456	143.2723173	738 ± 16	1281 ± 16
19AK-71	61.6739	-154.28194	829	2.9	0.964221	5.311E-16	50099.05015	931.3376906	5589 ± 104	-3570 ± 104
19AK-72	61.67412	-154.28212	828	2.5	0.964221	5.311E-16	29637.11618	480.6872695	3310 ± 54	-1291 ± 54
19AK-73	61.6741	-154.28217	828	2.2	0.964221	7.685E-16	4385.101937	133.2234875	485 ± 15	1534 ± 15
19AK-74	61.67403	-154.28236	832	2.67	0.964221	7.685E-16	8583.385857	173.1031463	948 ± 19	1071 ± 19
LH-3										
19AK-65	61.67059	-154.27878	864	2.77	0.964245	5.311E-16	19444.87589	362.2517703	2099 ± 39	-80 ± 39
19AK-66	61.67073	-154.27852	863	2.83	0.964245	5.311E-16	2829.863666	139.6079792	304 ± 15	1715 ± 15
19AK-67	61.67073	-154.27855	862	2.04	0.964245	5.311E-16	6728.670658	187.8287506	720 ± 20	1299 ± 20
19AK-68	61.67081	-154.27794	862	2.82	0.964245	5.311E-16	5635.083173	144.6010205	607 ± 16	1412 ± 16
19AK-69	61.67096	-154.27766	865	2.38	0.964245	5.311E-16	3192.530872	111.873276	342 ± 12	1677 ± 12

Notes: All rock density assumed 2.65 g/cm³. Zero surface erosion. Ages presented using the Arctic Production rate from Young et al. (2013) and Lm scaling (Lal, 1991; Stone, 2000). Please find all metadata presented in this table in the ICE-D database here: www.ice-d.org.

145

While the sampling techniques discussed above greatly reduce the likelihood of post-depositional processes impacting age determinations, it is virtually impossible to detect in the field which samples may have excessive cosmogenic nuclide inventories (i.e., nuclide inheritance) from surface exposure prior to glacier advances and moraine building events. Commonly with erosive (non-cold based) alpine glaciers, measured samples on moraines impacted by nuclide inheritance manifest as extreme values that do not conform with any other ages in the distribution. Thus, we suspect all samples observed on our three moraines with extreme old values that do not conform with any other ages were impacted by nuclide inheritance. Not considering the older extreme values across the three moraines (n = 5), we find 8 of the remaining 10 samples overlapping in two clusters, ~1200-1300 CE (n = 6) and ~1700 CE (n = 2). We tentatively conclude that because these samples are both internally consistent and consistent with other independent records of LIA glacier fluctuations in Alaska, they may reflect the true age of two LIA glacier advances at our site.

155

4 Climate change in the Revelation Mountains through deglaciation

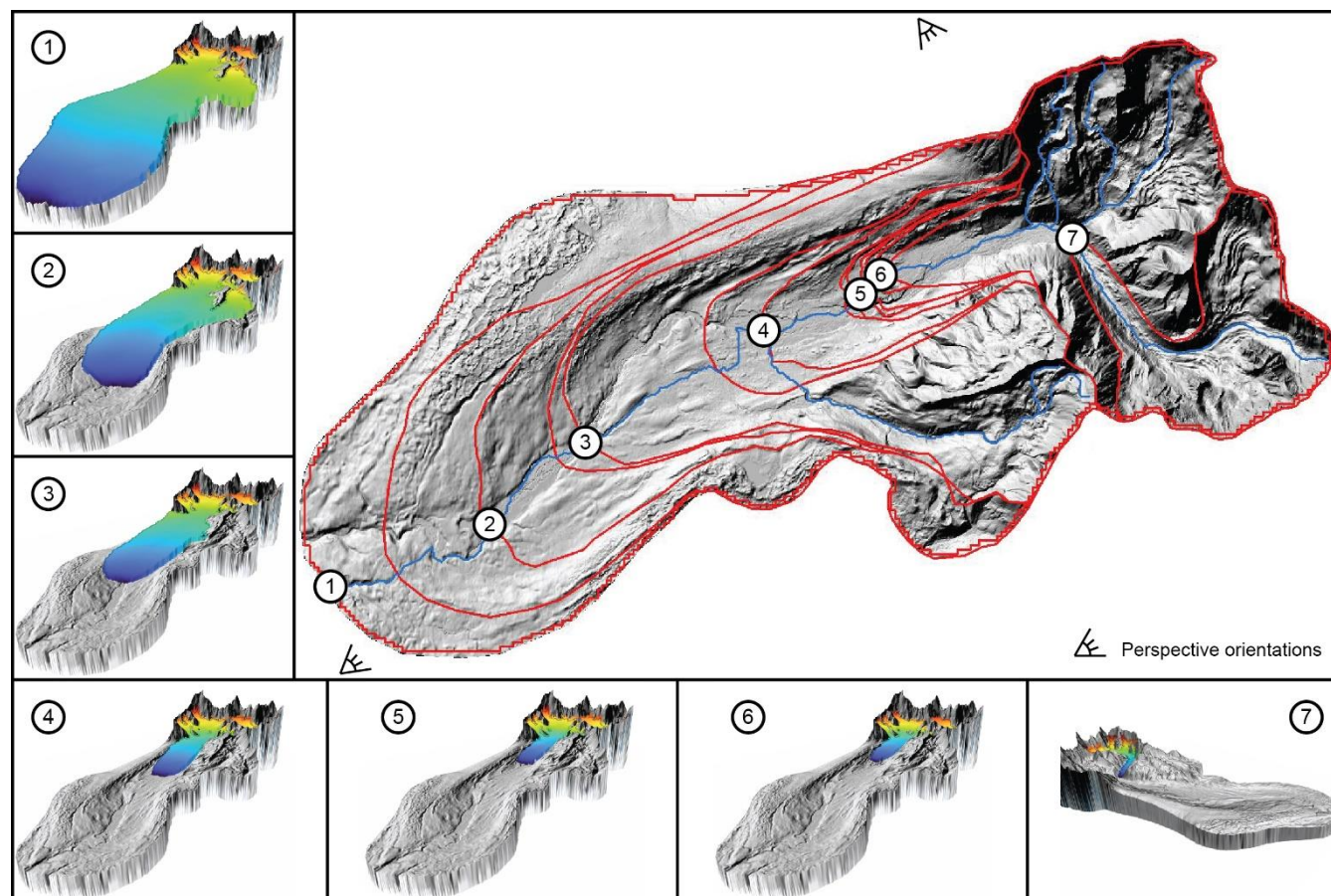
To construct a climate record built on the completed chronology at our site, we employ the tools developed for use in ArcGIS from Pelitiero et al. (2015, 2016) to first reconstruct paleo-glacier surfaces and then equilibrium line altitudes (ELAs) for each of the previously dated moraine positions (n = 14) and the outermost late Holocene moraine position (LH-1; 15 total moraines). We select the outermost late Holocene moraine because it is the most robustly dated and the late Holocene moraines are all within 1 km of each other, resulting in similar paleo ELA values. The glacier surface reconstruction tool

160



(GLARE; Pelitero et al., 2016) is semi-automated but requires the following inputs: a base map digital elevation model (DEM), polygons of maximum glacier outline constraints, and glacier center flowline polygons (Fig. 6). We mapped glacier outlines on a 5-meter resolution IFSAR DEM basemap provided by the USGS and available for download at the National Map (<https://apps.nationalmap.gov/downloader/>). Maximum constraints for each individual paleo-glacier position were outlined based on terminal and lateral moraines originally mapped in Tulenko et al., (2018), and extending up to the valley drainage divide in the steeper terrain once moraines were no longer visible. In steeper terrain, it is difficult to find preserved evidence of glacier extents, so the divide offers the maximum possible limit of glacial extent. For the remaining steps, we resampled the 5-meter resolution DEM down to 100-meter resolution to smooth out the surface. We suggest that since post-glacial landscape evolution has likely altered the land surface at fine scale, a smoothed surface may minimize any influence of post-glacial landscape evolution on our glacier surface reconstructions. Using the resampled DEM and the series of watershed analysis tools in ArcGIS, we produced ice flowline polylines that generally follow the modern drainages (Fig. 6). The GLARE tool then calculates ice thickness along the center flowline assuming perfect plasticity for ice rheology and a value for basal shear stress that we set to 1 hPa for all paleo-glaciers at all positions along their center flowlines. Finally, we use the topo to raster interpolation method (see Hutchinson et al., 2011 for details) supplied by the GLARE tool to reconstruct a glacier surface extending outward from center flowline thickness values of each paleo-glacier and confined either by their respective glacier outline where moraines exist or the valley wall in steeper terrain (see fig. 6 insets for examples).

Following glacier surface reconstructions, we employ the Accumulation Area Ratio method supplied by the ArcGIS ELA tool (Pelitero et al., 2015) for each paleo-glacier. We assume a ratio of 0.63 ± 0.04 , which has been suggested as representative for alpine glaciers greater than 4 km^2 (Kern and Laszlo, 2010). ELA values for each glacier position, along with age constraints reported in Tulenko et al. (2022) can be found in Table 2. Finally, we calculate summer temperature anomalies for each glacier position relative to the LIA by applying the dry adiabatic lapse rate of $10^\circ\text{C}/\text{km}$ to each ΔELA . The dry adiabatic lapse rate is applied because it serves as an endmember; over timescales greater than a few hours, it is not possible for an air mass to sustainably exceed the dry adiabatic lapse rate. Thus, our reconstruction likely provides a maximum estimate in the magnitude of temperature change at each glacier position because lower lapse rates would translate to smaller changes in atmospheric temperature.



190

195

Figure 6. Plan view of the North Swift River valley and reconstructed glacier extents in the main panel. Outlines of every glacier surface/extent reconstructed in this analysis (in red). Blue lines are the flowlines reconstructed on the resampled, lower-resolution DEM. In the insets are 3D visualizations of reconstructed glacier surfaces. ELA reconstructions at each glacier position viewed in oblique 3D with 4X vertical exaggeration. Each number in the main panel corresponds to the toe of the glacier position reconstructed in each inset panel. Glacier surfaces 1-6 are viewed from the perspective in the bottom left corner of the main panel and glacier surface 7 is viewed from the perspective near the top right.

200

205

Our ELA reconstructions indicate ~400 m of total ELA rise through the deglacial interval (975 m asl – 1362.5 m asl), which translates to approximately 4°C of warming (Fig. 7, Table 2). While there was notable lateral recession between 21-16 ka, the valley floor here is low-sloping, and we observe minimal ELA rise (~50 m) and modest warming (~0.4°C). Following this interval, a period of abrupt ELA rise corresponding to ~1.5°C of warming occurred, followed by a pause in deglaciation ~16-15 ka when several moraines were deposited. After this period, a second interval of net ~2°C warming from ~15 to 12.8 ka led to glacier recession and non-deposition of moraines until the final late glacial moraine preserved in our valley was deposited at 12.8 ± 0.6 ka with an ELA of 1362.5 m asl, only 16 m below the ELA of the outermost late Holocene moraine in the valley.



Table 2. Glacier equilibrium line altitude information.

Moraine name	Mean ELA (m)	ELA error (m)	Moraine age (ka)	Moraine age error (ka)
F2-I A	975	16	21.3	0.8
F2-I B	1019	18	20.1	1.3
F2-II A	1028	14	19.5	1.0
F2-II B	1030	14	18.7	0.8
F2-III A	1031	13	16.9	1.2
F2-III B	1043	18	16.0	0.9
F2-III C	1072	20	15.9	0.9
F2-III D	1141	22	16.6	0.6
F2-III E	1152	23	15.7	0.7
F2-IV A	1172	23	16.1	0.9
F2-IV B	1175.5	23.5	15.0	0.7
F2-IV C	1182.5	23.5	15.5	0.7
F2-IV D	1206	26	15.7	0.7
F2-IV E	1362.5	20.5	12.8	0.6
LH-1	1378.5	20.5	0.76	0.05

Notes: All ELAs are measured using 0.63 ± 0.04 Accumulation Area Ratios. All ages reported here are calculated in Tulenko et al. (2022).

210 5 Discussion

Given that modern average lapse rates in Alaska may be as low as $\sim 4.3^\circ\text{C}/\text{km}$ (Verbyla and Kurkowski, 2019), temperature estimates through the last deglaciation could be less than half the magnitude reported here (2°C total warming through deglaciation). However, additional proxy evidence across Alaska spanning deglaciation from pollen assemblages (Viau et al., 2008), fossil chironomids (Kurek et al., 2009), and leaf wax hydrogen isotope data (Daniels et al., 2021) – as well as Gulf
 215 of Alaska sea surface temperatures (Praetorius et al., 2020) – suggest $\sim 4^\circ\text{C}$ summer temperature depressions during the LGM, consistent with the glacier-based temperature reconstruction from the Revelation Mountains. Several data assimilation products based on marine sediment records further substantiate the magnitude of cooling observed in our record (Tierney et al., 2020). Moreover, multiple lines of proxy evidence from Alaska indicate conditions were drier than present through much of the last deglaciation until the late YD (Viau et al., 2008; Finkenbinder et al., 2014, 2015; Dorfman et al., 2015),
 220 suggesting the time-averaged late Pleistocene environmental lapse rate was likely higher than modern and closer to the endmember dry lapse rate used here. If the notable increase in precipitation observed following the YD (e.g., Viau et al.,



2008; Kaufman et al., 2010) had played a significant role in modulating glacier advances, we might have expected additional late glacial-to-Holocene moraines in our valley. Yet, as discussed later, any moraines that may have been deposited were overridden by subsequent LIA advances. Thus, agreeability in the magnitude of LGM cooling between our record and others
225 across Alaska, and the robustness of the lapse rate chosen for our study give us confidence in the magnitude of warming we reconstruct through deglaciation in the Revelation Mountains.

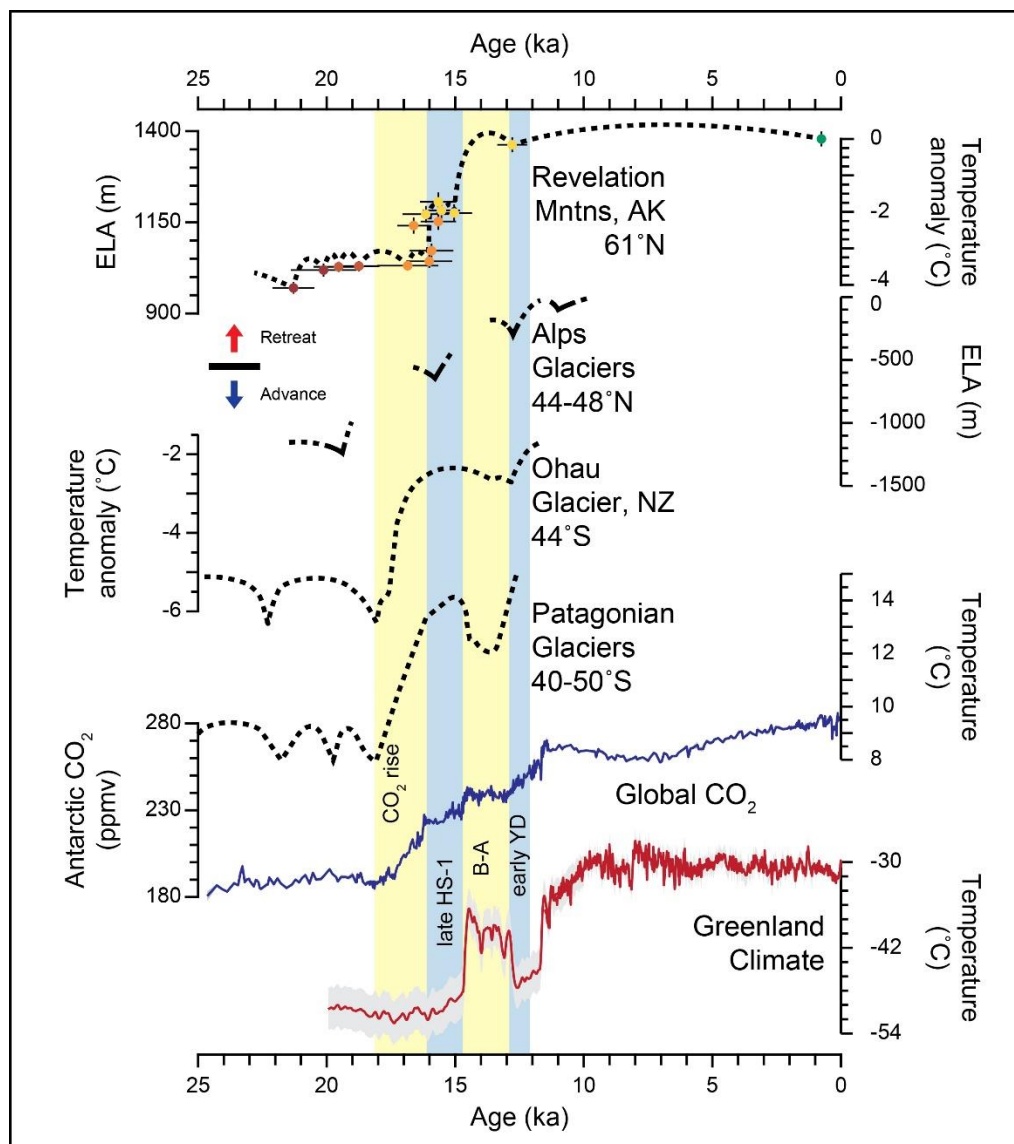
Moraine ages from across Alaska reveal an emerging pattern, although in no other valley is the moraine record as complete or well dated as in the Revelation Mountains. The Last Glacial Maximum advance culminated in Alaska ~21-19 ka
230 (Kaufman et al., 2011, Tulenko et al., 2018). Additionally, several moraines have been dated between ~16-15 ka during the later stage of Heinrich Stadial 1 (HS-1). In rare cases, most notably in the Revelation Mountains and in the Ahklun Mountains (e.g., Young et al., 2019), moraines date to ~12.8-12.1 ka during the late glacial and within the earliest and coldest interval of the Younger Dryas (YD). Despite limited chronologic constraints, the magnitude of glacier retreat observed in other valleys in Alaska appears to track with glaciers in the Revelation Mountains (Tulenko et al., 2022). Thus, it
235 is possible the last deglaciation climate reconstruction from the Revelation Mountains may be representative of the broader Alaska region.

Following the last deglaciation, we observe minimal glacier activity at our site through much of the Holocene until the LIA, when glacier advances nearly matched the extent of the youngest late glacial advance. While this is consistent with glacier
240 behavior at several sites in Alaska, we note the contrasting pattern of Holocene glacier activity observed in valleys in the Brooks Range. Observations suggest that some neoglacial advances predating the LIA were slightly more extensive in the region (e.g., Ellis and Calkin, 1984; Badding et al., 2013; Pendleton et al., 2017). Moreover, in the Ahklun Mountains, Young et al. (2019) observe two minor glacier re-advances in the Waskey valley at 12.5 ± 0.1 ka and 12.1 ± 0.4 ka. While there appears to be no preserved evidence of glacier advances between the 12.8 ± 0.6 ka moraine and the LIA moraines in
245 the Revelation Mountains, it is possible that minor advances occurred and were overridden by subsequent advances during the LIA. Regardless, late glacial-to-Holocene moraines deposited in Alaska narrowly exceed LIA advances indicating that late glacial and Holocene cooling events were minor in Alaska. Indeed, the Revelation Mountains record indicates less than 0.1° C temperature difference between early YD cooling and LIA cooling. So, while North Atlantic climate oscillations may be more strongly expressed during winter compared to summer (e.g., Bromley et al., 2018), our temperature record – along
250 with moraine dates at other sites – suggests North Atlantic climate forcings extend to Alaska.

In the context of detailed glacier reconstructions observed elsewhere around the world, we find both similarities and differences between our record and others (Fig. 7). Broadly, Southern Hemisphere glacier records indicate a coupling with global CO_2 reflected in Antarctic ice core records, while glaciers in Alaska follow patterns of alpine glacier recession in the
255 Alps and climate fluctuations recorded in Greenland Ice Cores (Fig. 7). Even if rising global CO_2 forced major recession



following deposition of the 17-ka moraine (F2-IIIa) and any evidence was overridden by subsequent moraine deposition events at our site, that scenario would still require a large magnitude re-advance during HS-1 in Alaska based on our record. While evidence for YD advances in Alaska extend beyond our site (Young et al., 2019), we acknowledge that within the resolution of ^{10}Be dating, the late glacial moraine at our site may have been deposited at the time of the Antarctic Cold Reversal ‘breakpoint’ like records in the Southern Hemisphere and a site in Norway (Putnam et al., 2023). Despite uncertainty in the age assignment of one moraine at our site, we still observe a dampened climate response in Alaska at intervals generally tracking North Atlantic climate oscillations – cooling and moraine deposition at the culmination of HS-1, retreat through the Bølling warm period and slight cooling during the early YD (Fig. 7) – with substantial deviation from records in the Southern Hemisphere, which all reinforces the notion that the North Atlantic signature of climate evolution through deglaciation extended out to Alaska.



270 **Figure 7. Comparison of the Revelation Mountains retreat chronology with Southern Hemisphere and Alps glacial retreat, and global/regional climate forcing mechanisms. Top to bottom: the Revelation Mountains ELA-based temperature curve (this study), composite ELA reconstructions from the Alps (Ivy-Ochs, 2015), temperature curve from Ohau Glacier, NZ (Putnam et al., 2013), composite temperature curve from Patagonian Glaciers (Denton et al., 1999; Strelin et al., 2011), composite atmospheric CO₂ concentrations from Antarctic Ice Cores (Bereiter et al., 2015), and Greenland-wide average mean annual temperature from ice cores (20-11 ka; Buizert et al., 2014, 11-0 ka; Kobashi et al., 2017).**

6 Conclusions

275 New ¹⁰Be ages from late Holocene moraines in the Revelation Mountains reveal similar culminations with other, well-dated records in southern Alaska at ~1200-1300 CE and ~1700 CE, suggesting similar climatic controls across southern and



western Alaska. The ELA-based temperature record from the Revelation Mountains, pinned by the late Holocene moraine constraints, indicates an LGM temperature depression of $\sim 4^{\circ}\text{C}$ relative to the LIA, consistent with other limited proxy data from across the state. Most warming was delayed following global CO_2 rise until ~ 16 ka when abrupt, $\sim 1.5^{\circ}\text{C}$ of warming forced significant retreat. Brief intervals of cooling and moraine deposition late during HS-1 and in the early YD interrupted the overall pattern of warming and glacier retreat, similar to the observed glacial records in the Alps. Paired with $\sim 2^{\circ}\text{C}$ of warming and glacier recession during the Bølling, these observations highlight the potential influence of North Atlantic forcing on climate in Alaska.

Data availability

All observations necessary to re-calculate ^{10}Be exposure ages are reported in the main text, as well as in the ICE-D online database (www.ice-d.org).

Author Contribution

JPT was responsible for conceptualization, formal analyses, visualizations and writing of the original draft for this manuscript. JPB, NEY, and JMS provided resources, funding acquisition, conceptualization, and review and editing of the original draft.

Competing interests

The authors declare that they have no conflict of interest.

Acknowledgements

We would like to acknowledge that samples in this study were collected on ancestral lands of the Dënëndeh and Dena'ina Elmena and that the University at Buffalo exists on the land of the Seneca. These peoples are the traditional caretakers of these lands. We give thanks for the opportunity to exist and work on lands that are rightfully theirs. We thank R. Schwartz for lab processing and LLNL for ^{10}Be measurements. Young and Schaefer acknowledge support from the LDEO Climate Center. This manuscript was supported by NSF grant 2135466.

References

Badding, M. E., Briner, J. P., and Kaufman, D. S.: ^{10}Be ages of late Pleistocene deglaciation and Neoglaciation in the north-central Brooks Range, Arctic Alaska, *Journal of Quaternary Science*, 28, 95–102, <https://doi.org/10.1002/jqs.2596>, 2013.



- 305 Balco, G., Stone, J. O., Lifton, N. A., and Dunai, T. J.: A complete and easily accessible means of calculating surface exposure ages or erosion rates from ^{10}Be and ^{26}Al measurements, *Quaternary geochronology*, 3, 174–195, 2008.
- Balco, G., Briner, J., Finkel, R. C., Rayburn, J. A., Ridge, J. C., and Schaefer, J. M.: Regional beryllium-10 production rate calibration for late-glacial northeastern North America, *Quaternary Geochronology*, 4, 93–107, 2009.
- 310 Barclay, D. J., Wiles, G. C., and Calkin, P. E.: Holocene glacier fluctuations in Alaska, *Quaternary Science Reviews*, 28, 2034–2048, <https://doi.org/10.1016/j.quascirev.2009.01.016>, 2009.
- Bereiter, B., Eggleston, S., Schmitt, J., Nehrbass-Ahles, C., Stocker, T. F., Fischer, H., Kipfstuhl, S., and Chappellaz, J.: Revision of the EPICA Dome C CO_2 record from 800 to 600 kyr before present, *Geophysical Research Letters*, 42, 542–549, 2015.
- 315 Braithwaite, R. J.: Temperature and precipitation climate at the equilibrium-line altitude of glaciers expressed by the degree-day factor for melting snow, *Journal of Glaciology*, 54, 437–444, <https://doi.org/10.3189/002214308785836968>, 2008.
- 320 Briner, J. P., Kaufman, D. S., Manley, W. F., Finkel, R. C., and Caffee, M. W.: Cosmogenic exposure dating of late Pleistocene moraine stabilization in Alaska, *Geological Society of America Bulletin*, 117, 1108–1120, 2005.
- Bromley, G., Putnam, A., Borns Jr, H., Lowell, T., Sandford, T., and Barrell, D.: Interstadial Rise and Younger Dryas Demise of Scotland’s Last Ice Fields, *Paleoceanography and Paleoclimatology*, 33, 412–429, <https://doi.org/10.1002/2018PA003341>, 2018.
- 325 Buizert, C., Gkinis, V., Severinghaus, J. P., He, F., Lecavalier, B. S., Kindler, P., Leuenberger, M., Carlson, A. E., Vinther, B., and Masson-Delmotte, V.: Greenland temperature response to climate forcing during the last deglaciation, *Science*, 345, 1177–1180, 2014.
- 330 Claude, A., Ivy-Ochs, S., Kober, F., Antognini, M., Salcher, B., and Kubik, P. W.: The Chironico landslide (Valle Leventina, southern Swiss Alps): age and evolution, *Swiss Journal of Geosciences*, 107, 273–291, 2014.
- 335 Daniels, W. C., Russell, J. M., Morrill, C., Longo, W. M., Giblin, A. E., Holland-Stergar, P., Welker, J. M., Wen, X., Hu, A., and Huang, Y.: Lacustrine leaf wax hydrogen isotopes indicate strong regional climate feedbacks in Beringia since the last ice age, *Quaternary Science Reviews*, 269, 107130, <https://doi.org/10.1016/j.quascirev.2021.107130>, 2021.



- 340 Denton, G. H., Lowell, T., Heusser, C., Schlüchter, C., Andersen, B. G., Heusser, L. E., Moreno, P. I., and Marchant, D. R.:
Geomorphology, stratigraphy, and radiocarbon chronology of Llanquihue Drift in the area of the Southern Lake District,
Seno Reloncaví, and Isla Grande de Chiloé, Chile, *Geografiska Annaler: Series A, Physical Geography*, 81, 167–229, 1999.
- Dorfman, J., Stoner, J., Finkenbinder, M., Abbott, M., Xuan, C., and St-Onge, G.: A 37,000-year environmental magnetic
record of aeolian dust deposition from Burial Lake, Arctic Alaska, *Quaternary Science Reviews*, 128, 81–97, 2015.
- 345 Dortch, J. M., Owen, L. A., Caffee, M. W., and Brease, P.: Late Quaternary glaciation and equilibrium line altitude
variations of the McKinley River region, central Alaska Range, *Boreas*, 39, 233–246, 2010.
- Ellis, J. M. and Calkin, P. E.: Chronology of Holocene glaciation, central Brooks range, Alaska, *Geological Society of
America Bulletin*, 95, 897–912, 1984.
- 350 Finkenbinder, M., Abbott, M., Finney, B., Stoner, J., and Dorfman, J.: A multi-proxy reconstruction of environmental
change spanning the last 37,000 years from Burial Lake, Arctic Alaska, *Quaternary Science Reviews*, 126, 227–241, 2015.
- Finkenbinder, M. S., Abbott, M. B., Edwards, M. E., Langdon, C. T., Steinman, B. A., and Finney, B. P.: A 31,000 year
record of paleoenvironmental and lake-level change from Harding Lake, Alaska, USA, *Quaternary Science Reviews*, 87, 98–
355 113, 2014.
- Hugonnet, R., McNabb, R., Berthier, E., Menounos, B., Nuth, C., Girod, L., Farinotti, D., Huss, M., Dussailant, I., Brun, F.,
and Kääb, A.: Accelerated global glacier mass loss in the early twenty-first century, *Nature*, 592, 726–731,
<https://doi.org/10.1038/s41586-021-03436-z>, 2021.
- 360 Hutchinson, M. F., Xu, T., and Stein, J. A.: Recent progress in the ANUDEM elevation gridding procedure,
Geomorphometry, 2011, 19–22, 2011.
- Ivy-Ochs, S.: Glacier variations in the European Alps at the end of the last glaciation, *Cuadernos de investigación
geográfica/Geographical Research Letters*, 295–315, 2015.
- 365 Kaufman, D. S., Anderson, R. S., Hu, F. S., Berg, E., and Werner, A.: Evidence for a variable and wet Younger Dryas in
southern Alaska, *Quaternary Science Reviews*, 29, 1445–1452, 2010.



- 370 Kaufman, D. S., Young, N. E., Briner, J. P., and Manley, W. F.: Alaska Palaeo-Glacier Atlas (Version 2), in: *Developments in Quaternary Sciences*, vol. 15, edited by: Ehlers, J., Gibbard, P. L., and Hughes, P. D., Elsevier, 427–445, <https://doi.org/10.1016/B978-0-444-53447-7.00033-7>, 2011.
- Kern, Z. and László, P.: Size specific steady-state accumulation-area ratio: an improvement for equilibrium-line estimation
375 of small palaeoglaciers, *Quaternary Science Reviews*, 29, 2781–2787, 2010.
- Kobashi, T., Menviel, L., Jeltsch-Thömmes, A., Vinther, B. M., Box, J. E., Muscheler, R., Nakaegawa, T., Pfister, P. L.,
Döring, M., and Leuenberger, M.: Volcanic influence on centennial to millennial Holocene Greenland temperature change,
Scientific reports, 7, 1441, 2017.
- 380 Kurek, J., Cwynar, L. C., Ager, T. A., Abbott, M. B., and Edwards, M. E.: Late Quaternary paleoclimate of western Alaska
inferred from fossil chironomids and its relation to vegetation histories, *Quaternary Science Reviews*, 28, 799–811, 2009.
- Lal, D.: Cosmic ray labeling of erosion surfaces: in situ nuclide production rates and erosion models, *Earth and Planetary
385 Science Letters*, 104, 424–439, 1991.
- Matmon, A., Briner, J., Carver, G., Bierman, P., and Finkel, R.: Moraine chronosequence of the Donnelly Dome region,
Alaska, *Quaternary Research*, 74, 63–72, 2010.
- 390 Nishiizumi, K., Imamura, M., Caffee, M. W., Southon, J. R., Finkel, R. C., and McAninch, J.: Absolute calibration of ^{10}Be
AMS standards, *Nuclear Instruments and Methods in Physics Research Section B: Beam Interactions with Materials and
Atoms*, 258, 403–413, <https://doi.org/10.1016/j.nimb.2007.01.297>, 2007.
- Oerlemans J.: Extracting a Climate Signal from 169 Glacier Records, *Science*, 308, 675–677,
395 <https://doi.org/10.1126/science.1107046>, 2005.
- Ohmura, A., Kasser, P., and Funk, M.: Climate at the Equilibrium Line of Glaciers, *Journal of Glaciology*, 38, 397–411,
<https://doi.org/10.3189/S0022143000002276>, 1992.
- 400 Palacios, D., Stokes, C. R., Phillips, F. M., Clague, J. J., Alcalá-Reygosa, J., Andrés, N., Angel, I., Blard, P.-H., Briner, J. P.,
and Hall, B. L.: The deglaciation of the Americas during the Last Glacial Termination, *Earth-Science Reviews*, 203, 103113,
2020.



- Pellitero, R., Rea, B. R., Spagnolo, M., Bakke, J., Hughes, P., Ivy-Ochs, S., Lukas, S., and Ribolini, A.: A GIS tool for
405 automatic calculation of glacier equilibrium-line altitudes, *Computers & Geosciences*, 82, 55–62,
<https://doi.org/10.1016/j.cageo.2015.05.005>, 2015.
- Pellitero, R., Rea, B. R., Spagnolo, M., Bakke, J., Ivy-Ochs, S., Frew, C. R., Hughes, P., Ribolini, A., Lukas, S., and
410 Renssen, H.: GlaRe, a GIS tool to reconstruct the 3D surface of palaeoglaciers, *Computers & Geosciences*, 94, 77–85,
<https://doi.org/10.1016/j.cageo.2016.06.008>, 2016.
- Pendleton, S. L., Briner, J. P., Kaufman, D. S., and Zimmerman, S. R.: Using Cosmogenic ^{10}Be Exposure Dating and
Lichenometry to Constrain Holocene Glaciation in the Central Brooks Range, Alaska, *Quaternary Science Reviews*, 173, 115–132,
<https://doi.org/10.1657/AAAR0016-045>, 2017.
415
- Praetorius, S. K., Condrón Alan, Mix Alan C., Walczak Maureen H., McKay Jennifer L., and Du Jianghui: The role of
Northeast Pacific meltwater events in deglacial climate change, *Science Advances*, 6, eaay2915,
<https://doi.org/10.1126/sciadv.aay2915>, 2020.
- 420 Putnam, A. E., Schaefer, J. M., Denton, G. H., Barrell, D. J., Birkel, S. D., Andersen, B. G., Kaplan, M. R., Finkel, R. C.,
Schwartz, R., and Doughty, A. M.: The last glacial maximum at 44 S documented by a ^{10}Be moraine chronology at Lake
Ohau, Southern Alps of New Zealand, *Quaternary Science Reviews*, 62, 114–141, 2013.
- Putnam, A. E., Bromley, G. R., Rademaker, K., and Schaefer, J. M.: In situ ^{10}Be production-rate calibration from a ^{14}C -
425 dated late-glacial moraine belt in Rannoch Moor, central Scottish Highlands, *Quaternary Geochronology*, 50, 109–125,
2019.
- Putnam, A. E., Denton, G. H., and Schaefer, J. M.: A ^{10}Be chronology of the Esmark Moraine and Lysefjorden region,
southwestern Norway: Evidence for coeval glacier resurgence in both polar hemispheres during the Antarctic Cold Reversal,
430 *Quaternary Science Reviews*, 316, 108259, 2023.
- Roe, G. H., Baker, M. B., and Herla, F.: Centennial glacier retreat as categorical evidence of regional climate change, *Nature
Geoscience*, 10, 95–99, <https://doi.org/10.1038/ngeo2863>, 2017.
- 435 Rupper, S. and Roe, G.: Glacier changes and regional climate: a mass and energy balance approach, *Journal of Climate*, 21,
5384–5401, 2008.



- 440 Schaefer, J. M., Denton, G. H., Barrell, D. J., Ivy-Ochs, S., Kubik, P. W., Andersen, B. G., Phillips, F. M., Lowell, T. V., and
Schlüchter, C.: Near-synchronous interhemispheric termination of the last glacial maximum in mid-latitudes, *science*, 312,
1510–1513, 2006.
- Schaefer, J. M., Denton, G. H., Kaplan, M., Putnam, A., Finkel, R. C., Barrell, D. J., Andersen, B. G., Schwartz, R.,
Mackintosh, A., and Chinn, T.: High-frequency Holocene glacier fluctuations in New Zealand differ from the northern
signature, *science*, 324, 622–625, 2009.
- 445 Stone, J. O.: Air pressure and cosmogenic isotope production, *Journal of Geophysical Research: Solid Earth*, 105, 23753–
23759, 2000.
- Strelin, J., Denton, G., Vandergoes, M., Ninnemann, U., and Putnam, A.: Radiocarbon chronology of the late-glacial Puerto
450 Bandera moraines, southern Patagonian Icefield, Argentina, *Quaternary Science Reviews*, 30, 2551–2569, 2011.
- Tierney, J. E., Zhu, J., King, J., Malevich, S. B., Hakim, G. J., and Poulsen, C. J.: Glacial cooling and climate sensitivity
revisited, *Nature*, 584, 569–573, 2020.
- 455 Tulenko, J. P., Briner, J. P., Young, N. E., and Schaefer, J. M.: Beryllium-10 chronology of early and late Wisconsinan
moraines in the Revelation Mountains, Alaska: Insights into the forcing of Wisconsinan glaciation in Beringia, *Quaternary
Science Reviews*, 197, 129–141, <https://doi.org/10.1016/j.quascirev.2018.08.009>, 2018.
- 460 Tulenko, J. P., Briner, J. P., Young, N. E., and Schaefer, J. M.: The last deglaciation of Alaska and a new benchmark 10Be
moraine chronology from the western Alaska Range, *Quaternary Science Reviews*, 287, 107549, 2022.
- Valentino, J. D., Owen, L. A., Spotila, J. A., Cesta, J. M., and Caffee, M. W.: Timing and extent of Late Pleistocene
glaciation in the Chugach Mountains, Alaska, *Quaternary Research*, 101, 205–224, 2021.
- 465 Verbyla, D. and Kurkowski, T. A.: NDVI–Climate relationships in high-latitude mountains of Alaska and Yukon Territory,
Arctic, Antarctic, and Alpine Research, 51, 397–411, <https://doi.org/10.1080/15230430.2019.1650542>, 2019.
- Viau, A., Gajewski, K., Sawada, M., and Bunbury, J.: Low-and high-frequency climate variability in eastern Beringia during
the past 25 000 years, *Canadian Journal of Earth Sciences*, 45, 1435–1453, 2008.
- 470



- Wiles, G. C., Jacoby, G. C., Davi, N. K., and McAllister, R. P.: Late Holocene glacier fluctuations in the Wrangell Mountains, Alaska, *Geological Society of America Bulletin*, 114, 896–908, 2002.
- 475 Wiles, G. C., D'Arrigo, R. D., Villalba, R., Calkin, P. E., and Barclay, D. J.: Century-scale solar variability and Alaskan temperature change over the past millennium, *Geophysical Research Letters*, 31, 2004.
- Wittmeier, H. E., Schaefer, J. M., Bakke, J., Rupper, S., Paasche, Ø., Schwartz, R., and Finkel, R. C.: Late Glacial mountain glacier culmination in Arctic Norway prior to the Younger Dryas, *Quaternary Science Reviews*, 245, 106461, 2020.
- 480 Young, N. E., Schaefer, J. M., Briner, J. P., and Goehring, B. M.: A 10 Be production-rate calibration for the Arctic, *Journal of Quaternary Science*, 28, 515–526, 2013.
- Young, N. E., Briner, J. P., Schaefer, J., Zimmerman, S., and Finkel, R. C.: Early Younger Dryas glacier culmination in southern Alaska: Implications for North Atlantic climate change during the last deglaciation, *Geology*, 47, 550–554, 2019.